Journal of Materials Chemistry A

Accepted Manuscript

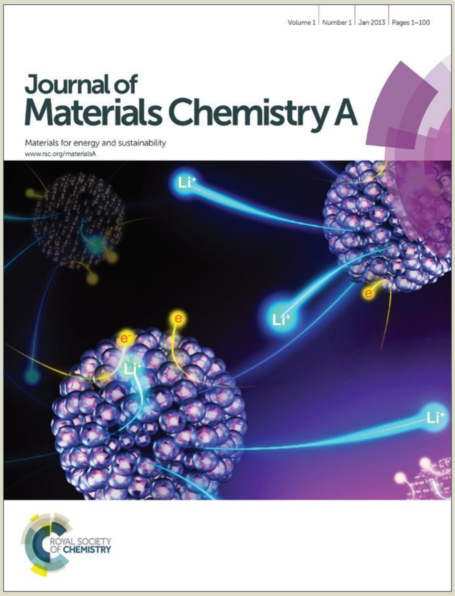

ROYAL SOCIETY OF CHEMISTRY

www.rsc.org/materialsA

Journal Name

ARTICLE

Synthesis of Modified Fullerenes for Oxygen Reduction Reactions

Rosa María Girón,[a] Juan Marco-Martínez,[a] Sebastiano Bellani,[b,c] Alberto Insuasty,[a] Hansel Comas Rojas,[b] Gabriele Tullii, [b] Maria Rosa Antognazza,[b,]* Salvatore Filippone,[a,]* and Nazario Martín[a,d,]*

Received 00th January 20xx,
Accepted 00th January 20xx

DOI: 10.1039/x0xx00000x

www.rsc.org/

Oxygen reduction reaction (ORR) is a key process common in several energy converting systems or electro-chemical technologies such as fuel cells, metal-air batteries, oxygen sensors, etc. which is based on the use of expensive and scarcely available platinum metal. In the search for carbon-based catalysts for ORR, two different classes of new fullerene hybrids and metal-free fullerene derivatives endowed with suitable active sites have been prepared by highly selective metal- and organo-catalyzed synthetic methodologies. Along with their classical behavior as electron acceptors in polymer-based photo-electrochemical cells, the new fullerene derivatives are able to efficiently catalyze ORRs by using no metals or very low amounts of metals. Remarkably, the activity of metal-free fullerenes has proved to be as high as that observed for metallofullerenes bearing noble metals, and up to ten-fold higher than that of PCBM.

Introduction

Oxygen reduction reaction (ORR) is a key process in different energy converting systems or electrochemical technologies (fuel cells, metal air batteries, oxygen sensors, etc).[1] In these fields the replacement of the traditional platinum based catalysts with non-precious metals[2] or metal-free electrocatalysts is currently a hot scientific challenge.[3] Particularly, the use of carbon nanomaterials such as nitrogen-doped carbon nanotubes[4] or graphene,[5] represents an interesting and novel approach.

In this context, among the different allotropic forms of carbon, fullerenes combine unique chemical,[6] optical,[7] electronic[8] and photophysical[9] properties with a defined molecular structure. Indeed, their good electron accepting and transport capability led to their extended use as suitable n-type materials,[10] widely employed in organic electronics and photovoltaic devices,[11] including the most recent perovskites solar cells.[12]

Thus, bulk heterojunction (BHJ) organic photovoltaic cells (OPV) are a notable application, which consist of p-type conjugated polymers (e.g. poly(3-hexylthiophene-2,5-diyl), P3HT) and n-type fullerene derivatives, being [6,6]phenyl-C_{61}-butyric acid methyl ester (PCBM) the most widely used. In a typical BHJ approach, a bi-continuous network is created, which allows to promote exciton dissociation processes and to achieve a high power conversion efficiency. The next frontier in the use of acceptor/donor BHJs, based on PCBM, is the realization of photo-electrochemical cells, able to work in contact with aqueous and/or non-aqueous electrolytes upon visible light illumination. One notable example is the realization of efficient photocathodes for hydrogen production by photo-electrochemical water splitting.[13],[14] Recently, some of us have reported a high sensitivity, photo-electrochemical oxygen sensor based on an organic BHJ formed by a low band gap polymer (APFO-3) and PCBM, revealing photo-activity towards ORR.[15] In the proposed scheme, polymer excitation by visible light leads to the efficient generation of bounded charged species (excitons), which are promptly dissociated into free charges (polarons) by highly efficient electron transfer process to the fullerene-based acceptors domain. We have recently reported that this process, typical of solid-state photovoltaic cells, occurs in the hybrid system with fully comparable dynamics and efficiency.[16] Photogenerated holes are collected at the underlying fluorine-doped tin oxide (FTO) electrode, while electrons are efficiently transferred at the interface with the aqueous solution, thus giving rise to photoelectrochemical reactions and, in particular, to ORR (Figure 1).

Here, we report the synthesis of new fullerene derivatives, suitably functionalized with catalytic active sites towards ORR. This allows us to exploit a doubled fullerenes functionality, by employing them both as electron acceptors in P3HT-based BHJ, and as redox active sites, thus avoiding the use of expensive noble metals.

---

[a] *Departamento de Química Orgánica I, Facultad de Ciencias Químicas, Universidad Complutense de Madrid, Ciudad Universitaria s/n, 28040 Madrid (Spain); E-mail: salvatorefilippone@ucm.es; E-mail: nazmar@quim.ucm.es.*
[b] *.Center for Nano Science and Technology @PoliMi, Istituto Italiano di Tecnologia, Via Pascoli 70/3, 20133 Milano, Italy; E-mail: mariarosa.antognazza@iit.it*
[c] *Istituto Italiano di Tecnologia, Graphene Labs, Via Morego 30, Genova 16163, Italy*
[d] *IMDEA-Nanociencia, Campus de la Universidad Autónoma de Madrid, 28049 Madrid (Spain).*

† Footnotes relating to the title and/or authors should appear here.

Electronic Supplementary Information (ESI) available: [details of any supplementary information available should be included here]. See DOI: 10.1039/x0xx00000x

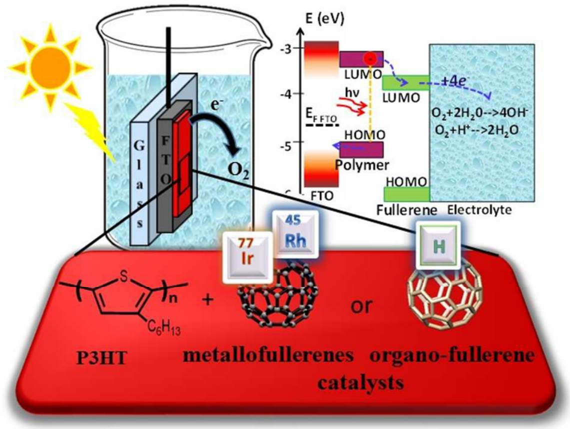

Figure 1. Schematic sketch of an organic-based photo-electrochemical device for ORR, based on P3HT:fullerene BHJ thin films. The working mechanism and the energetic levels schemes are also represented.

Two main approaches have been undertaken in parallel: i) the synthesis of new fullerene hybrid derivatives endowed with noble metals active in redox processes, such as Ir, Rh or Pt; ii) the synthesis of metal-free fullerene catalysts, based on the presence of active C_{60}-H bonds. To this aim, both metal- and organo-catalytic methodologies have been employed, to obtain fullerene derivatives with tailored electronic and photocatalytic properties characterized by high regio- and stereo-selectivity.

Photoelectrochemical devices for ORR based on BHJ P3HT:fullerenes thin films have been finally realized, confirming an enhanced photocatalytic property of the novel compounds, when compared with the extensively used PCBM, taken as the reference fullerene.

2. Results and Discussions

2.1. Synthesis of metallo- and organo-fullerenes catalysts

Over the last years, fullerene chemistry has been widening its synthetic tools′ in the search for more sophisticated structures,[17] for a better control on the stereochemistry of the fullerene derivatives[18] and for a control on the regio- and site-selectivity when higher fullerenes[19] or endohedrals[20] are used. Following this trend, on one hand, we have directed our attention to the achievement of new selective catalytic methodologies aimed to the preparation of both metallo-fullerenes and regiopure fullerene hydrides. On the other hand, we have modified both metal- and organo-catalysed methodologies,[21] previously described by us, for the introduction on the fullerene cage of the suitable functionality to become catalytically active towards ORR.

2.1.1. Pyrrolino-metallo-fullerenes

With the aim of preparing stable metallo-fullerene hybrids, we firstly directed our attention onto iridium (III) complexes due to their wide use in hydrogenation processes and for their ability to form stable and easily isolable complexes. Thus, the design of the iridium-fullerene complexes were based on the preparation of pyrrolino[60]fullerene ligands endowed with a carboxylic group to bind efficiently iridium(III) as well as other active metals. To this purpose, we carried out the 1,3-dipolar cycloaddition reaction of azlactone **1** onto [60]fullerene by using a racemic silver BINAP catalyst, followed by the addition of the iridium dimer $[Cp^*IrCl_2]_2$ (see Scheme 1). A unique compound, **1Ir**, was obtained in "one-pot" and in good yield (*ca*. 40%) as a result of two sequential processes where two chiral centers are formed: in the first step, a pyrrolino[3,4:1,2][60]fullerene carboxylic acid is formed with a stereogenic center in the C-5 of the pyrroline ring. In the second process, iridium(III) is covalently linked diastereoselectively to the [60]fullerene derivative through the formation of two new bonds, one with the nitrogen of the pyrroline ring and the other one with the oxygen of the carboxylate group. The presence of the metal is confirmed by the IR spectrum of the isolated solid, since the ν(CO) of the starting pyrroline shifts from 1700 cm^{-1} to 1660 cm^{-1} in the final product, which is in agreement with the previously observed behaviour of fullerene-iminocarboxylate as (N, O)-chelating monoanionic ligands.[22] It is worthy to note that, despite iridium(III), with its typical pseudo-tetrahedral geometry, could adopt two possible configurations and, therefore, affording a diastereomeric mixture, the overall process occurs diastereoselectively, in sharp contrast to other related examples.[23]

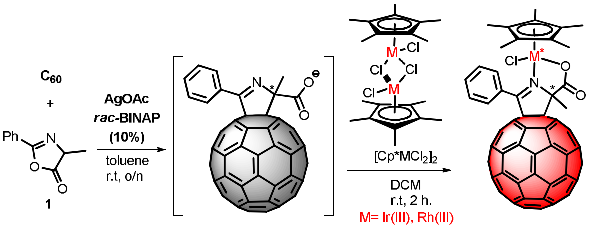

2Ir (40%, *d.e.*>99:1)
2Rh (38%, *d.e.*>99:1)

Scheme 1. Diastereomeric synthesis of iridium (**2Ir**) and rhodium (**2Rh**) pyrrolino[3,4:1,2][60]fullerene.

Indeed, this behaviour was observed by ^{1}H-NMR (see supporting information) and its structure could be confirmed by X-ray diffraction analysis of a monocrystal obtained by slow evaporation of **2Ir** in CS_2/hexane.[24]

As it is shown in Figure 2, the iridium atom adopts a pseudo octahedral geometry where Cp* group occupies a face of the octahedron, being 1.775 Å the distance between the metal and the ring centroid. Two other octahedron positions involve the chelate pyrrolinofullerene carboxylate featuring an Ir-N, Ir-O bonds of 2.103(4) Å and 2.095(4) Å length, respectively. Finally, the determined Ir-Cl bond distance resulted to be 2.393(2) Å, which is slightly shorter than other related pyrrolidinocarboxilate Iridiun Cp* complexes.[23b] The distance between the two sphere *sp*^{3} carbon atoms is 1.590(8) Å, which is in the typical range for a fullerene monoadduct.

X-Ray analysis confirms the presence of a single diastereomer (with both enantiomers) with the chlorine atom in a *trans* position to the methyl group of the iridium cycle (see also supporting information).

Analogously, a rhodium pyrroline[60]fullerene hybrid **2Rh** was prepared in 38% yield, by using [Cp*RhCl$_2$]$_2$ after the cycloaddition of the same azlactone **1** (Scheme 1).

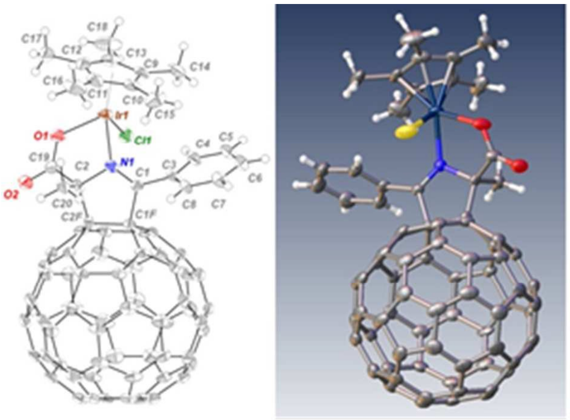

Figure 2. X-Ray diffraction of a crystal of **2Ir** obtained by slow evaporation in CS$_2$/hexane.

2.1.2. Organocatalytic synthesis of metal-free fullerene catalyst

Fullerenes with their 30 (for C$_{60}$) or more strained C = C double bonds have been envisaged as very useful molecular species for hydrogen storage and, therefore, fullerene hydrides (or fulleranes) have been deeply studied.[25],[26] Furthermore, these species easily undergo dehydrogenation in the presence of even very low amount of molecular oxygen.[27] In this regard, we wondered if the presence of highly active hydrogen directly linked to the carbon cage could replace precious metals but still maintaining a high catalytic activity. Thus, we designed a regioselective double addition on [60]fullerene where a C$_{60}$-H bond is formed by the use of organocatalytic methodology. To this aim, we extended the scope of our previously reported phosphine catalyzed cycloaddition of allenoates/alkynoates to [60]fullerene[21b, 28] to 5-hydroxy-3-alkynoates (Scheme 2).

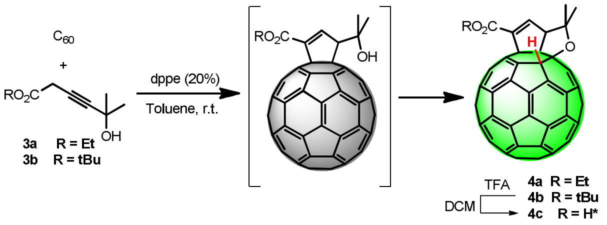

Scheme 2. *Cis*-1 regioselective fullerene bifunctionalization affording fullerene hydrides.

Thus, after alkynoate/allenoate isomerization, 1,2-diphenylphosphino ethane (dppe) catalysed Lu's [3+2] cycloaddition[29] of **3a,b** affording the corresponding cyclopentenoate[60]fullerene. These products are not isolated since they underwent an easy regioselective addition of the hydroxyl group to the *cis*-1 double bond of C$_{60}$ giving rise to bisadducts **4a,b** endowed with a C$_{60}$-H bond in 48% and 34% yields, respectively. Eventually, the corresponding acid **4c** was obtained after acidic removal of *tert*-butyl ester.

2.2. Photocatalytic activity of fullerene derivatives toward ORR in photoelectrochemical devices

The new fullerene derivatives were finally tested as photo-electrocatalysts in polymer-based devices for photo-electrochemical ORR, and overall electrochemical performances were compared to devices employing PCBM as a standard reference material. Used compounds are classified in Chart 1 into three main types: fullerenes without catalytic sites, but with higher-lying LUMO levels compared to PCBM, as mere acceptor components (**DPM-12** and **bisDPM-12,** in grey colour, top panel); hybrid fullerenes with metallic catalytic sites (**2Ir**, **2Rh** and **6** compounds, in red) and catalytic, metal-free fullerenes (**4a**, **4b** and **4c** compounds, in green).

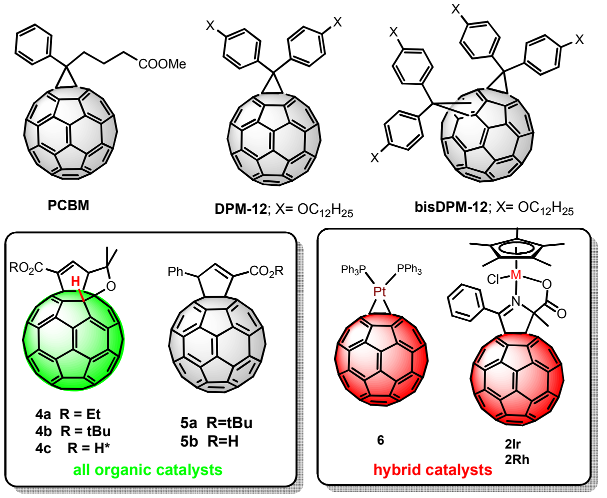

Chart 1. Fullerene derivatives used as acceptors/catalysts in photo-electrochemical devices.

BHJ thin films (~140 nm), based on rr-P3HT as photoactive donor component, were deposited by spin coating on top of FTO-covered glass substrates. In some cases, a second thin film fullerene layer was deposited on top of the photoactive component, in order to directly expose catalytic sites to the electrolyte. Photo-catalytic activity towards oxygen reduction was assessed in sodium phosphate buffer (PBS) at pH 7.4 and controlled dissolved oxygen (DO) concentration (5.8 mg/L). All details about materials absorbance spectra, device fabrication processing, experimental set up and measurement conditions are reported in the SI section.

Figure 3 reports Linear Scan Voltammetry (LSV) recorded in dark and upon illumination (1 SUN) in devices based on fullerene acceptors without any catalytic site (PCBM, **DPM-12** and **bisDPM-12**).

As demonstrated in a previous work,[15] the recorded current signal can be unambiguously attributed to photo-activated electrochemical reactions occurring at the hybrid organic/electrolyte interface and in particular to ORR (see also Figure S2 in the supporting information section). Moreover, dark current values (dashed lines) are negligible in all cases.

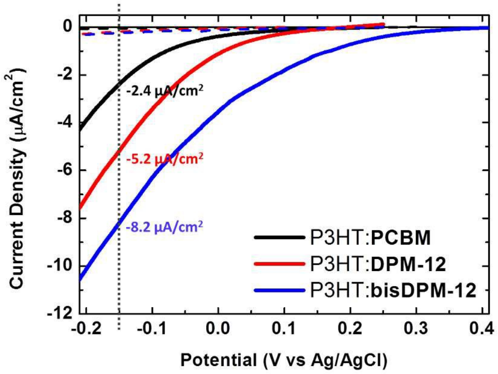

Figure 3. Linear Scan Voltammetry (LSV) measurements under dark (dashed lines) and upon visible light (1 SUN) (solid lines) on FTO/ P3HT:fullerenes (PCBM, DPM-12 and bisDPM-12) photo-electrochemical cells (scan rate, 10 mV/s). Measurements were performed in sodium phosphate buffer (PBS) at pH 7.4 and controlled dissolved oxygen (DO) concentration (5.8 mg/L).

Notably, the use of **DPM-12** and **bisDPM-12** fullerene bisadducts allows to increase the Onset Potential (OP, defined here as the voltage at which the photocurrent density amounts at 100 nA/cm^2) up to 0.15 V vs. Ag/AgCl and 0.35 V vs. Ag/AgCl, respectively, with respect to the reference PCBM, 0.12 V vs. Ag/AgCl. Correspondingly, at a fixed voltage the photocurrent density increases: at -0.15 V vs. Ag/AgCl, for instance, it amounts at -2.4 μA/cm^2, -5.2 μA/cm^2, -8.2 μA/cm^2 for PCBM, **DPM-12** and **bisDPM-12,** respectively. An analogous behavior has also been reported in organic solar cells, where an increase of the open circuit voltage in the case of **DPM-12** and **bisDPM-12** was reported, when compared to PCBM.[30] The enhanced performances are possibly attributed to the broader density of states and to the higher-lying LUMO level of the fullerene bisadducts, able to facilitate the electron transfer processes occurring at the organic/electrolyte interfaces.

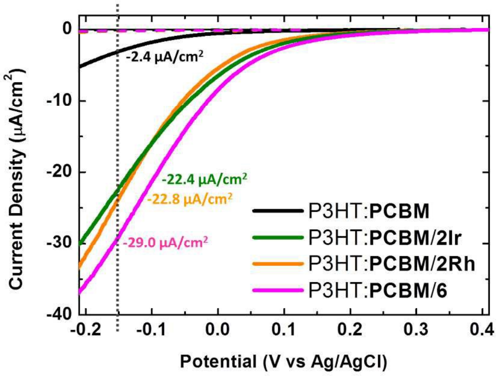

Figure 4. Hybrid fullerenes, endowing metallic catalytic sites, for ORR. Linear Scan Voltammetry (LSV) measurements (scan rate, 10 mV/s) under dark (dashed lines) and upon visible light (1 SUN) (solid lines) on FTO/ P3HT:PCBM/hybrid catalyst (**2Ir**, **2Rh** and **6**) photo-electrochemical cells. Measurements were performed in sodium phosphate buffer (PBS) at pH 7.4 and controlled dissolved oxygen (DO) concentration (5.8 mg/L).

Iridium, rhodium and platinum are known to be efficient catalysts for ORR.[31] Hybrid catalysts, **2Ir**, **2Rh** and **6**, are thus expected to provide catalytic properties typical of the embedded metal component, but with a consistently reduced need of precious metals, and with the advantage of a more localized interaction. In this case photo-electrodes were realized by covering the reference P3HT:PCBM BHJ layer with an over-layer of pristine electron acceptor, in order to maximize the localization at the electrolyte interface of the catalytic sites endowed within the functionalized fullerene derivatives (P3HT:PCBM/hybrid catalyst configuration).

The adopted strategy resulted to be successful. All tested hybrid catalysts show photocurrent density values larger of more than one order of magnitude with respect to reference PCBM, and comparable dark current values (Figure 4). Photocurrent generation is clearly related to the presence of dissolved oxygen, and its origin can be safely attributed to the occurrence of ORR(see supporting information, Figure S4, panels a and b,). OPs are also considerably increased, shifting from 0.12 V vs Ag/AgCl for PCBM up to 0.3 V vs Ag/AgCl for **2Ir** and **2Rh** and to 0.35V vs Ag/AgCl for **6**. Reported data allow to conclude that electrons can be easily transferred towards metallic catalytic centres which, in turn are highly efficient in reducing the overpotential needed to foster ORR. In other words, the use of hybrid fullerenes endowed with catalytic centres increases both the electron transfer rate (observed as a net photocurrent density increase) and the driving force for electrochemical reactions (observed as OP increase).

On the other hand, following the recent trend for using carbon based materials as catalyst in ORR,[3-5] we planned the preparation of a molecular organocatalyst by replacement of the metallic atoms from the fullerene derivatives, with a fullerene hydride as active site. The choice of using catalysts such as **4a-c** relies on the reported hydrogen transfer from the fullerene hydrides, namely $C_{60}H_2$, to dioxygen[27] and on the easy deprotonation of fullerene hydrides leading to very stable fullerene anions **4**$^-$.[26]

In order to evaluate the importance of the hydrogen fullerene bond, devices based on analogous cyclopentenoate functionalization but lacking the C_{60}-H bond (**5a,b)** were also prepared.

Figure 5 summarizes the results obtained in the characterization of photo-electrochemical cells based on **4a**, **4b**, **4c**, **5a** and **5b** components as hybrid electron acceptor/catalysts components, as compared to the reference device based on PCBM**.**

We notice that **4a** leads to higher catalytic activity, with more than 5-folds increase in photocurrent density at -0.15 V vs Ag/AgCl respect to PCBM, and a higher OP value (0.3V vs Ag/AgCl). Conversely, **5a** and **5b**, despite presenting a similar cyclopentenoate moiety on the C_{60} cage, they do not show a significative increase of the performance due to the lack of C_{60}-H bond. While **5a** exhibits a similar behaviour to PCBM, the higher hydrophilicity of **5b**, bearing a carboxylic acid group, leads to a closer interaction with dissolved oxygen molecules, which could explain the higher photocurrent densities observed in **5b**.

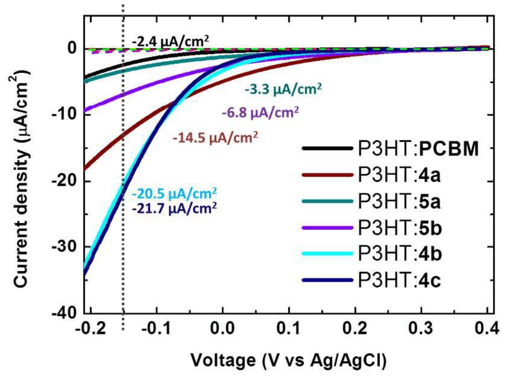

Figure 5. Use of metal-free fullerene catalysts for ORR. Linear Scan Voltammetry (LSV) measurements (scan rate, 10 mV/s) under dark (dashed lines) and upon visible light (1 SUN) (solid lines) on FTO/ P3HT:fullerene catalysts (**4a**, **5a**, **5b**, **4b** and **4c**). Measurements were performed in sodium phosphate buffer (PBS) at pH 7.4 and controlled dissolved oxygen (DO) concentration (5.8 mg/L).

Finally, we further functionalized **5a** and **5b** compounds by directly linking the active hydrogen to the carbon cage, as in the case of the more efficient **4a** compound, obtaining **4b** and **4c**, respectively. Once more, photocurrent generation is related to the occurrence of ORR (see supporting information, Figure S4, panel c). Additional measurements in O_2-saturated conditions on **4b** and **4c** are shown in the supporting information (Figure S5). These data have now been compared with those based on PCBM. Importantly, recorded photocurrent densities for **4b** and **4c** show values comparable to the ones obtained for the hybrid catalysts P3HT:PCBM/**2Ir** and P3HT:PCBM/**2Rh**, in the order of -20 $\mu A/cm^2$ at -0.15 V vs Ag/AgCl. OPs resulted 0.28 V in both cases which are still lower respect to the ones of precious metal hybrid samples (0.3 V vs Ag/AgCl for PCBM/2Ir and 0.35 V vs Ag/AgCl for PCBM/2Rh and PCBM/6) suggesting future efforts to increment the cell's voltage efficiency with these catalytic materials. Despite of this, metal-free fullerene samples showed higher durability respect to the precious metal hybrid samples. As figure of merit, the photocurrents recorded at -0.2V vs Ag/AgCl for consecutive Cyclic Voltammetry (CV) cycles have been taken (see supporting information, Figure S6). At the fortieth cycle a decrease of the photocurrent of 12.9%, 21.2% and 45.4%, respect to the value recorded at the first cycle, is observed for the case of PCBM, **4c** and **6**, respectively. Interestingly, while for PCBM and **4c** photocurrent reached stable values after few cycles of stabilization, for the case of **6** a progressively decrease is observed, probably as a consequence of detrimental effects. This could be due to different ORR mechanisms for the hybrid catalyst when compared to the other cases. As a matter of fact, for Pt electrode two-electron reduction of oxygen to H_2O_2 occurs parallel to the four-electron reduction to H_2O (see supporting information, Scheme S1). Consequently, a decrease of the cell voltage could arise because of the lower reversible redox potential of H_2O_2. Similar effects have been also reported in durability studies of fuel cells.[32]

Regarding the catalitic activity of the metal-free fullerene derivatives **4a-c**, a plausible mechanism to account for the photocurrent increase and observed stability is based on the initial transfer of the photo-generated electron (PET) from the polymer to catalysts **4a-c** affording the corresponding fullerene radical anion (Scheme 3). Thus, an easier oxygen reduction takes place to form the hydroperoxyl radical, through a hydrogen atom transfer (HAT) or by a proton coupled electron transfer (PCET), driven by the formation of the highly stable fullerene anions **4**$^-$.

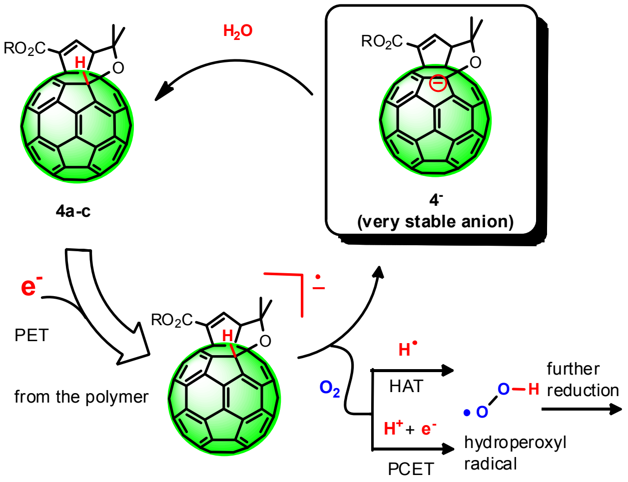

Scheme 3. Plausible ORR mechanism involving fullerene organocatalysts.

These overall results clearly show that it is possible to obtain comparable results to the hybrid catalysts through multiple metal-free functionalization, taking advantage from the positive roles in increasing catalytic activity towards ORR by each organo-modification of the fullerene cage.

Conclusions

In summary, we have reported the highly selective catalytic synthesis of two series of fullerene-based molecular catalysts for ORR. Iridium and rhodium pyrrolinofullerene complexes were prepared with a complete diastereoselectivity (*d.e.* >99%) and the structure of the iridium-fullerene complex was confirmed by X-ray analysis. On the other hand, metal-free fullerene catalysts, endowed with a highly active C_{60}-H bond, have been obtained by a regioselective *cis-1* addition to the C_{60} cage. The electrocatalytic activity versus the oxygen reduction reactions has been tested in bulk heterojunction photo-electrochemical cells, affording current values up to ten fold higher than widely used PCBM. Remarkably, metal-free fullerene derivatives proved to give photocurrents comparable to related hybrids, thanks to the highly active C_{60}-H bond on the fullerene cage. Future efforts have still to focus on improving their OPs, thus increasing the voltage efficiency of coming cells based on these carbon materials.

Acknowledgements

We acknowledge the financial support of the European Community through the Future and Emerging Technologies (FET) programme under the FP7, collaborative Project contract no. 309223 (PHOCS). NM thanks the European Research Council ERC-2012-ADG_20120216 (Chirallcarbon), MINECO of Spain (CTQ2014-52045-R) and the CAM (FOTOCARBON project S2013/MIT-2841). R. M. G thanks to Ministerio de Educación, Cultura y Deporte for the FPU contract.

Notes and references

Experimental details for the preparation of the fullerene derivatives, polymer blends absorption spectra, spectroscopic and chromatographic data for characterization of compounds, Linear Scan Voltammetry and Cyclic Voltammetry (CV) measurements are available in the supporting information.

CCDC 960717 contains the supplementary crystallographic data for this paper. These data can be obtained free of charge from The Cambridge Crystallographic Data Centre via www.ccdc.cam.ac.uk/data_request/cif.

1. (a) B. C. H. Steele and A. Heinzel, *Nature*, 2001, **414**, 345-352; (b) F. Cheng and J. Chen, *Chem. Soc. Rev.*, 2012, **41**, 2172-2192.
2. Z. Chen, D. Higgins, A. Yu, L. Zhang and J. Zhang, *Energy Environ. Sci.*, 2011, **4**, 3167-3192.
3. (a) L. Dai, Y. Xue, L. Qu, H.-J. Choi and J.-B. Baek, *Chem. Rev.*, 2015, **115**, 4823-4892; (b) D.-W. Wang and D. Su, *Energy Environ. Sci.*, 2014, **7**, 576-591.
4. K. Gong, F. Du, Z. Xia, M. Durstock and L. Dai, *Science*, 2009, **323**, 760-764.
5. (a) D. Higgins, P. Zamani, A. Yu and Z. Chen, *Energy Environ. Sci.*, 2016, **9**, 357-390; (b) J. Guan, X. Chen, T. Wei, F. Liu, S. Wang, Q. Yang, Y. Lu and S. Yang, *J. Mater. Chem. A*, 2015, **3**, 4139-4146.
6. A. Hirsch and M. Brettreich, *Fullerenes: Chemistry and Reactions*, Wiley VCH Weinheim, Germany, 2005.
7. L. W. Tutt and A. Kost, *Nature*, 1992, **356**, 225-226.
8. L. Echegoyen and L. E. Echegoyen, *Acc. Chem. Res.*, 1998, **31**, 593-601.
9. D. M. Guldi and M. Prato, *Acc. Chem. Res.*, 2000, **33**, 695-703.
10. J. E. Anthony, A. Facchetti, M. Heeney, S. R. Marder and X. Zhan, *Adv. Mater.*, 2010, **22**, 3876-3892.
11. (a) J. L. Delgado, P.-A. Bouit, S. Filippone, M. A. Herranz and N. Martin, *Chem. Commun.*, 2010, **46**, 4853-4865; (b) B. C. Thompson and J. M. J. Fréchet, *Angew. Chem. Int. Ed.*, 2008, **47**, 58-77.
12. (a) A. Abrusci, S. D. Stranks, P. Docampo, H.-L. Yip, A. K. Y. Jen and H. J. Snaith, *Nano Lett.*, 2013, **13**, 3124-3128; (b) P.-W. Liang, C.-C. Chueh, S. T. Williams and A. K. Y. Jen, *Adv. Energy Mater.*, 2015, **5**, n/a-n/a.
13. (a) F. Fumagalli, S. Bellani, M. Schreier, S. Leonardi, H. C. Rojas, A. Ghadirzadeh, G. Tullii, A. Savoini, G. Marra, L. Meda, M. Gratzel, G. Lanzani, M. T. Mayer, M. R. Antognazza and F. Di Fonzo, *Journal of Materials Chemistry A*, 2016, **4**, 2178-2187; (b) T. Bourgeteau, D. Tondelier, B. Geffroy, R. Brisse, R. Cornut, V. Artero and B. Jousselme, *ACS Appl. Mater. Interfaces*, 2015, **7**, 16395-16403; (c) M. Haro, C. Solis, G. Molina, L. Otero, J. Bisquert, S. Gimenez and A. Guerrero, *J. Phys. Chem. C*, 2015, **119**, 6488-6494; (d) G. M. Suppes, P. J. Fortin and S. Holdcroft, *J. Electrochem. Soc.*, 2015, **162**, H551-H556; (e) M. P. Gustafson, N. Clark, B. Winther-Jensen and D. R. MacFarlane, *Electrochim. Acta*, 2014, **140**, 309-313.
14. H. Comas Rojas et al under review
15. S. Bellani, A. Ghadirzadeh, L. Meda, A. Savoini, A. Tacca, G. Marra, R. Meira, J. Morgado, F. Di Fonzo and M. R. Antognazza, *Adv. Funct. Mater.*, 2015, **25**, 4531-4538.
16. A. Guerrero, M. Haro, S. Bellani, M. R. Antognazza, L. Meda, S. Gimenez and J. Bisquert, *Energy Environ. Sci.*, 2014, **7**, 3666-3673.
17. N. Martín, M. Altable, S. Filippone and A. Martín-Domenech, *Synlett*, 2007, 3077.
18. E. E. Maroto, M. Izquierdo, S. Reboredo, J. Marco-Martínez, S. Filippone and N. Martín, *Acc. Chem. Res.*, 2014, **47**, 2660-2670.
19. E. E. Maroto, A. de Cózar, S. Filippone, Á. Martín-Domenech, M. Suarez, F. P. Cossío and N. Martín, *Angew. Chem. Int. Ed.*, 2011, **50**, 6060-6064.
20. (a) E. E. Maroto, J. Mateos, M. Garcia-Borràs, S. Osuna, S. Filippone, M. Á. Herranz, Y. Murata, M. Solà and N. Martín, *J. Am. Chem. Soc.*, 2015, **137**, 1190-1197; (b) E. E. Maroto, M. Izquierdo, M. Murata, S. Filippone, K. Komatsu, Y. Murata and N. Martín, *Chem. Commun.*, 2014, **50**, 740-742; (c) K. Sawai, Y. Takano, M. Izquierdo, S. Filippone, N. Martín, Z. Slanina, N. Mizorogi, M. Waelchli, T. Tsuchiya, T. Akasaka and S. Nagase, *J. Am. Chem. Soc.*, 2011, **133**, 17746-17752.
21. (a) J. Marco-Martínez, S. Reboredo, M. Izquierdo, V. Marcos, J. L. López, S. Filippone and N. Martín, *J. Am. Chem. Soc.*, 2014, **136**, 2897-2904; (b) J. Marco-Martínez, V. Marcos, S. Reboredo, S. Filippone and N. Martín, *Angew. Chem. Int. Ed.*, 2013, **52**, 5115-5119.
22. a) S.H. Laurie, in: G. Wilkinson (Ed.), Comprehensive Coordination Chemistry, vol. 2, Pergamon, Oxford, 1987, p. 739 (Chapter 20.2). b) K. Nakamoto, Infrared and Raman Spectra of Inorganic and Coordination Compounds, fourth ed. Wiley, New York, 1986, pp. 233.
23. a) W. Bauer, M. Prem, K. Polborn, K. Sünkel, W. Steglich and W. Beck, *Eur. J. Inorg. Chem.*, 1998, **1998**, 485-493. b) D. Carmona, M. Pilar Lamata, F. Viguri, E. San José, A. Mendoza, F. J. Lahoz, P. García-Orduña, R. Atencio and L. A. Oro, *J. Organomet. Chem.*, 2012, **717**, 152-163.
24. CCDC 960717 contains the supplementary crystallographic data for this paper. These data can be obtained free of charge from The Cambridge Crystallographic Data Centre via www.ccdc.cam.ac.uk/data_request/cif.
25. F. Cataldo and S. Iglesias-Groth, eds., *Fulleranes the Hydrogenated Fullerenes*, Springer Science+Business Media B.V., Dordrecht, 2010.
26. J. Nossal, R. K. Saini, L. B. Alemany, M. Meier and W. E. Billups, *Eur. J. Org. Chem.*, 2001, **2001**, 4167-4180.
27. G. W. Wang, Y. J. Li, F. B. Li and Y. C. Liu, *Lett. Org. Chem.*, 2005, **2**, 595-598.
28. R. M. Girón, S. Reboredo, J. Marco-Martínez, S. Filippone and N. Martín, *Faraday Discuss.*, 2014, **173**, 311-322.
29. C. Zhang and X. Lu, *J. Org. Chem.*, 1995, **60**, 2906-2908.
30. (a) A. Sánchez-Díaz, M. Izquierdo, S. Filippone, N. Martin and E. Palomares, *Adv. Funct. Mater.*, 2010, **20**, 2695-2700; (b) G. Garcia-Belmonte, P. P. Boix, J. Bisquert, M. Lenes, H. J. Bolink, A. La Rosa, S. Filippone and N. Martín, *J. Phys. Chem. Lett.*, 2010, **1**, 2566-2571; (c) Y.-J. Cheng, M.-H. Liao, C.-Y. Chang, W.-S. Kao, C.-E. Wu and C.-S. Hsu, *Chem. Mater.*, 2011, **23**, 4056-4062.
31. (a) D. Cao, A. Wieckowski, J. Inukai and N. Alonso-Vante, *J. Electrochem. Soc.*, 2006, **153**, A869-A874; (b) Y. Nie, L. Li and Z. Wei, *Chem. Soc. Rev.*, 2015, **44**, 2168-2201; (c) J. Qiao, R. Lin, B. Li, J. Ma and J. Liu, *Electrochim. Acta*, 2010, **55**, 8490-8497.
32. (a) J. Qiao, M. Saito, K. Hayamizu, T. Okada, *J. Electrochem. Soc.,* 2006, **15** , A967-A974; (b) V. A. Sethuraman, J. W. Weidner, A. T. Haug, M. Pemberton, L. V. Protsailo *Electrochimica Acta*, 2009, **54** , 5571-5582.

Suitably functionalized fullerenes bearing an active metal atom or just an active hydrogen atom behave simultaneously as electron acceptors in bulk heterojunction devices and as catalyst in ORR. Remarkably, metal-free fullerene derivatives proved to be as active as the related hybrids.